IOPscience iopscience.iop.org

Home Search Collections Journals About Contact us My IOPscience

Overview of recent HERMES results

This content has been downloaded from IOPscience. Please scroll down to see the full text.

2016 J. Phys.: Conf. Ser. 678 012038

(http://iopscience.iop.org/1742-6596/678/1/012038)

View the table of contents for this issue, or go to the journal homepage for more

Download details:

IP Address: 131.169.95.162
This content was downloaded on 09/01/2017 at 10:32

Please note that terms and conditions apply.

Overview of recent HERMES results

Hrachya Marukyan (On behalf of the HERMES Collaboration)
AANL (Yerevan Physics Institute), Alikhanian Brs. 2, Yerevan 036, Armenia
E-mail: marukyan@mail.desy.de

Abstract. An overview of more recent and important results from the HERMES experiment are presented in this paper. HERMES collected a wealth of data using the 27.6 GeV polarized HERA lepton beam and various polarized and unpolarized gaseous targets. This unique data set opens the door to the measurements of observables sensitive to the multidimensional structure of the nucleon. Among them are semi-inclusive deep-inelastic scattering measurements of azimuthal modulations sensitive to the transverse momentum distributions, such as the leading-twist Sivers and Collins distributions and distributions sensitive to the convolutions of the twist-2 and twist-3 functions. They all provide an information on the three-momentum-dependent quark distributions. Knowledge on the quark distribution as a function of longitudinal momentum and transverse position in impact-parameter space can be accessed, e.g., through exclusive $\omega-$meson leptoproduction, particularly through the measurement of spin density matrix elements and the measurement of azimuthal modulations on transversely polarized proton target. The measurement of Bose-Einstein correlations of hadron pairs in quasi-real leptoproduction are also presented. The transverse polarization of Λ hyperons measured again in quasi-real leptoproduction regime are presented as well. Finally, the new analysis for the search on pentaquark at HERMES are mentioned.

1. Introduction

The HERMES experiment at DESY collected data from 1995 until 2007 using the 27.6 GeV HERA lepton beam. In the experiment, longitudinally polarized electrons or positrons were scattered off longitudinally, transversely or unpolarized hydrogen targets, longitudinally polarized deuterium and helium targets and unpolarized deuterium, helium, or heavier nuclear targets. The scattered lepton and particles produced in the reaction were detected by a forward spectrometer. The lepton-hadron separation was performed using a transition-radiation detector, a scintillator preshower counter, an electromagnetic calorimeter and a threshold gas Cherenkov counter (ring-imaging Cherenkov detector from 1998). The lepton identification efficiency exceeds 98% with a hadron misidentification contamination below 1%. Hadon identification was performed by Cherenkov detectors, allowing the discrimination of pions, kaons and protons.

The analysis of the azimuthal distribution of hadrons in semi-inclusive deep-inelastic (DIS) of leptons off a transversely polarized hydrogen target provides access to the Sivers distribution [1] and Collins fragmentation [2] functions. The former describes the distribution of unpolarized quarks in a transversely polarized nucleon, correlating quark transverse momentum with the nucleon's transverse spin, while the latter the fragmentation of a transversely polarized quark into an unpolarized hadron. The selected results sensitive to these two quantities are presented in section 2. The results from the recent analysis of $\sin\phi_h$ amplitudes of single-spin asymmetry


Content from this work may be used under the terms of the Creative Commons Attribution 3.0 licence. Any further distribution of this work must maintain attribution to the author(s) and the title of the work, journal citation and DOI.
Published under licence by IOP Publishing Ltd

in semi-inclusive DIS leptoproduction of hadrons in case of collision of a longitudinally polarized lepton beam with an unpolarized target are also considered in this section.

Data collected on transversely polarized hydrogen target are used to extract the amplitudes of single-spin asymmetry of the cross section in hard exclusive electroproduction of $\omega-$ mesons. They provide information on the sign of $\pi\omega$ transition form factor. The measurement of amplitudes of azimuthal sine modulations are presented in section 3.

Data from deep-inelastic scattering of longitudinally polarized electrons and positrons off polarized ^{1}H, ^{2}H and ^{3}He targets and unpolarized ^{4}He, N, Ne, Kr and Xe nuclear targets are used to measure the Bose-Einstein correlations of like-sign charged hadrons. The polarized data were summed over the spin orientation. The measurement of these correlation are discussed in section 4.

Measurements of transverse polarization of Λ hyperons from quasi-real photoproduction in the scattering of longitudinally polarized electrons and positrons off longitudinally or transversely polarized hydrogen target and longitudinally polarized deuterium target are discussed in section 5. The direction of the target polarization was reversed in 1-3 min intervals, resulting in a vanishing average target polarization of the data set.

Finally, the renewed analysis for the search of the pentaquark signal again in the regime of quasi-real photoproduction are presented in section 6. In addition to further data from a deuterium target, data from hydrogen targets were used in the analysis and are presented here.

2. Single- and double-spin asymmetries measured in SIDIS on unpolarized and transversely polarized proton target

Semi-inclusive DIS off a transversely polarized target (T) allows to access the single- and double-spin asymmetry amplitudes with characteristic angular modulations. Two angles appear in the description of the cross section of this process: angle ϕ, denoting the angle between the lepton-scattering and the hadron-production planes, and ϕ_S, being the azimuthal angle of the transverse component of the target-spin vector about the virtual photon direction with respect to the lepton scattering plane. Each of the azimuthal amplitudes corresponds to convolutions of different distribution and fragmentation functions. Two of them, proportional respectively to the $\sin(\phi - \phi_S)$ and $\sin(\phi + \phi_S)$ modulations, are interpreted as the convolutions of the Sivers distribution function [1] and the spin-independent fragmentation function and transversity and the Collins fragmentation function [2]. The HERMES results on the Sivers and Collins amplitudes for charged and neutral pions and for charged kaons as a function of x, z and $P_{h\perp}$ were published in Ref. [3] and Ref. [4], respectively. Here, x represents the Bjorken scaling variable, z denotes the fractional hadron energy with respect to the virtual photon energy in the target rest frame and $P_{h\perp}$ the magnitude of the transverse momentum of the final state hadron. In figure 1 the preliminary results of the extracted Collins amplitudes projected in bins of x, z and $P_{h\perp}$ are presented for protons and antiprotons. The statistical (systematic) uncertainties are given as error bars (bands).

Moreover, the fine binned three-dimensional extraction of various azimuthal amplitudes for charged pions, kaons and protons are possible from HERMES data, in projection of above mentioned kinematic parameters, which allows to constrain global fits to the experimental measurements in a more profound way. As an example, in figure 2 and figure 3 are shown respectively the Collins amplitudes for negative pions and Sivers amplitudes for protons vs. x extracted for four z and $P_{h\perp}$ bins. The three-dimensional extraction of all possible single- and double-spin asymmetry amplitudes sensitive to different combination of distribution and fragmentation functions are also available (not shown here).

In case of longitudinal beam (L) and unpolarized target (U) only target spin-independent parts can contribute to the asymmetry. Here, the structure function of interest is related to the asymmetry amplitude $A_{LU}^{\sin\phi_h}$, which is sensitive to convolutions of twist-2 distribution

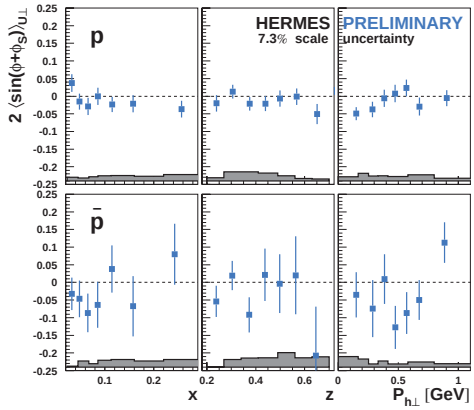

Figure 1. Collins amplitudes for protons and antiprotons as a function of x, z and $P_{h\perp}$.

(fragmentation) functions with twist-3 fragmentation (distribution) functions. HERMES published the results of single-spin asymmetry A_{LU} for charged and neutral pions as a function of x, z and $P_{h\perp}$ [5]. The multidimensional extraction of asymmetry amplitudes $A_{LU}^{\sin\phi_h}$ are shown in figure 4 and figure 5 respectively for negative and positive pions in projections of x, z and $P_{h\perp}$ in four bins for each of the kinematic variable.

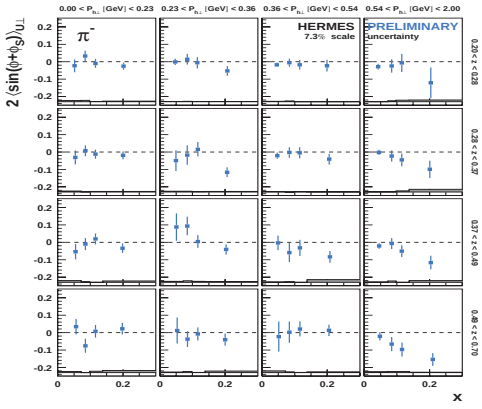

Figure 2. Collins amplitudes for π^- vs. x for four bins in z and $P_{h\perp}$.

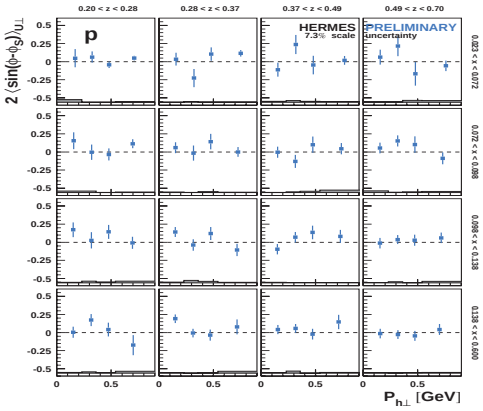

Figure 3. Sivers amplitudes for protons vs. x for four bins in z and $P_{h\perp}$.

3. Exclusive $\omega-$meson leptoproduction

Hard exclusive electroproduction of $\omega-$mesons is studied with the HERMES spectrometer by scattering longitudinally polarized positron and electron beams on unpolarized hydrogen and deuterium targets or on transversely polarized hydrogen target in the kinematic region

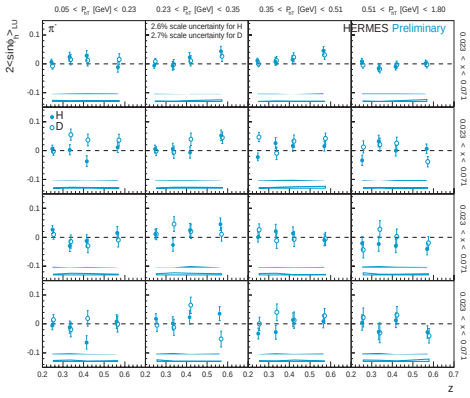

Figure 4. The multidimensional extraction of $A_{LU}^{\sin\phi_h}$ amplitudes for π^- mesons.

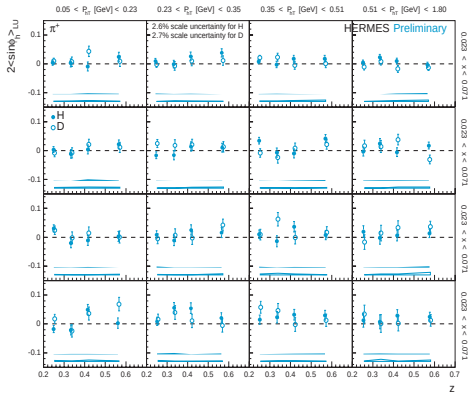

Figure 5. The multidimensional extraction of $A_{LU}^{\sin\phi_h}$ amplitudes for π^+ mesons.

$Q^2 > 1.0\,\mathrm{GeV}^2, 3.0\,\mathrm{GeV} < \mathrm{W} < 6.3\,\mathrm{GeV}$, and $-\mathrm{t}' < 0.2\,\mathrm{GeV}^2$. Here, Q^2 represents the negative square of the virtual-photon four-momentum, W is the invariant mass of the photon-nucleon system and $-t'$ is the smallest kinematically allowed value of the momentum transfer to the target. Using an un-binned maximum likelihood method, 15 unpolarized and 8 polarized Spin Density Matrix Elements (SDMEs) are extracted from unpolarized hydrogen and deuterium data [6]. From the analysis of transversely polarized hydrogen data the amplitudes of five sine modulations of the single-spin asymmetry of the cross section with respect to the transverse proton polarization are measured [7], the Q^2 and $-t'$ dependence of which are shown in figure 6. They are determined in the entire kinematic region (open squares) as well as for two bins in photon virtuality and momentum transfer to the nucleon (full circles). The inner error bars represent the statistical uncertainties, while the outer ones indicate the statistical and systematic uncertainties added in quadrature. The results receive an additional 8.2% scale uncertainty corresponding to the target polarization uncertainty. These results are compared to a phenomenological model that includes the pion pole contribution [8]. As can be seen from figure 6, within this model, the data favor a positive $\pi\omega$ transition form factor, the sign of which was not possible to determine from the measurements of SDMEs. Also, a separation of asymmetry amplitudes into longitudinal and transverse components is performed (not shown here).

4. Bose-Einstein correlations in hadron pairs from leptoproduction on nuclei

Bose-Einstein correlations of like-sign charged hadrons produced in deep-inelastic electron and positron scattering are studied in the HERMES experiment using nuclear targets of ^{1}H, ^{2}H, ^{3}He, ^{4}He, N, Ne, Kr, and Xe [9]. A Gaussian approach is used to parameterize a two-particle correlation function determined from events with at least two charged hadrons of the same sign charge. This correlation function is compared to two different empirical distributions that do not include the Bose-Einstein correlations. One distribution is derived from unlike-sign hadron pairs (method MUS), and the second from mixing like-sign pairs from different events (method MEM). The extraction procedure used simulations incorporating the experimental setup in order to correct the results for spectrometer acceptance effects, and was tested using the distribution of unlike-sign hadron pairs. Double ratio correlation function $R(T)$ for like-sign hadron pairs,

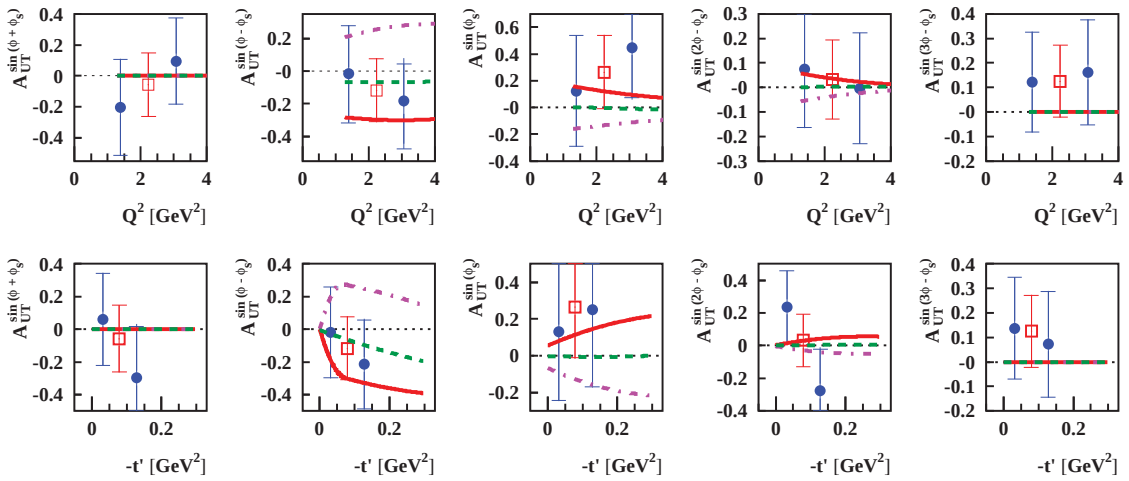

Figure 6. The amplitudes describing the strength of the sine modulations of the cross section for hard exclusive $\omega-$meson production.

obtained with above mentioned two methods from the hydrogen data are shown in figure 7, where T is the square of the difference of the two particle four-momenta. $W-$dependence of the particle source distribution size r_G (Goldhaber radius) and chaoticity parameter λ are shown respectively on top and bottom panels of figure 8. In figure 9 the world data on measured average value of r_G in lepton nucleon scattering experiments is plotted. No evidence for a dependence on W is found. The $A-$dependence of the parameters r_G (top panel) and λ (bottom panel) are shown in figure 10. Clear signals of Bose-Einstein correlations for all target nuclei without a significant variation with the nuclear target mass are found.

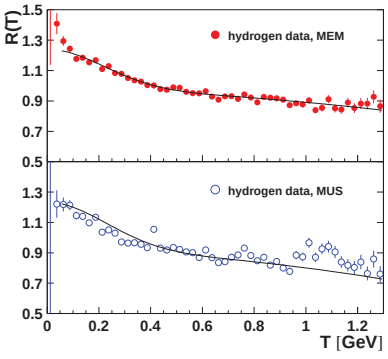

Figure 7. Double ratio correlation function for like-sign hadron pairs obtained with MEM and MUS based on hydrogen target data.

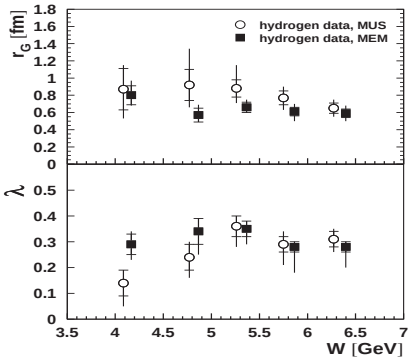

Figure 8. Parameter r_G (top panel) and λ (bottom panel) as a function of W, obtained with MEM and MUS methods on hydrogen.

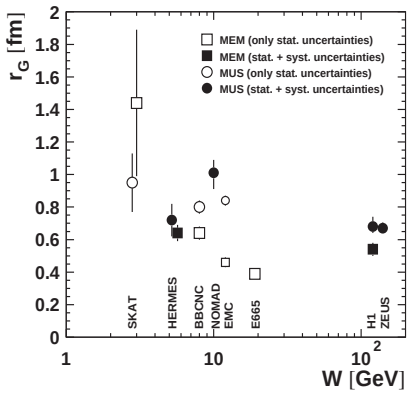

Figure 9. Goldhaber radius r_G, as a function of W, obtained in lepton nucleon scattering experiments.

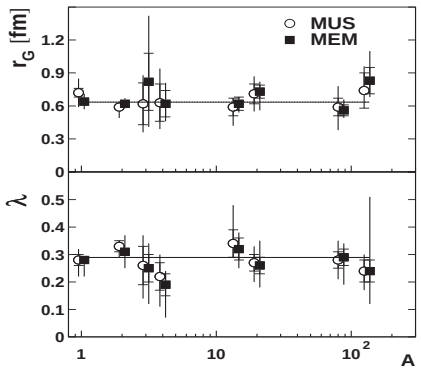

Figure 10. The parameters r_G and λ as a function of the target atomic mass A.

5. Transverse polarization of Λ hyperons from quasi-real photoproduction on nuclei

The transverse polarization of Λ hyperons was measured at HERMES [10] in inclusive quasi-real photoproduction for various target nuclei ranging from hydrogen to xenon. The dependence of the transverse polarization P_n^Λ on the atomic-mass number A of the target nuclei is shown in figure 11. As can be seen from this figure the measured polarization is positive for light target nuclei. It decreases with the atomic-mass number A of the target and is compatible with zero for heavier nuclei krypton and xenon. In figure 12 and figure 13 the dependence of the transverse polarization P_n^Λ is shown respectively as a function of the variable ζ and the transverse momentum p_T of the Λ hyperon for the combined hydrogen and deuterium data (closed symbols) and the combined krypton and xenon data (open symbols). Here, $\zeta = (E^\Lambda + p_L)/(E + k)$ with E^Λ and E being the energies of the produced Λ and the beam lepton, respectively, p_L the Λ's momentum component in the beam direction measured in the target rest frame, and k the lepton momentum. The error bars represent the statistical uncertainty. The values of $\langle p_T \rangle$ for each ζ bin and $\langle \zeta \rangle$ for each p_T bin are shown in the lower panels of corresponding figures.

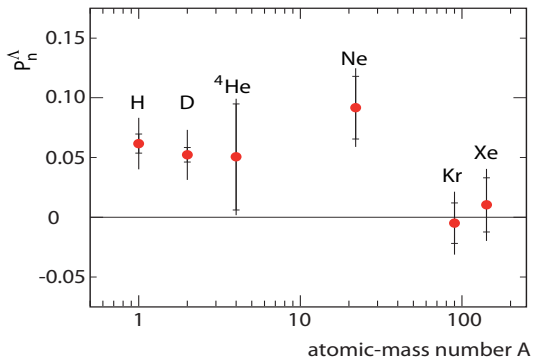

Figure 11. Dependence of the transverse polarization P_n^Λ on the atomic-mass number A of the target nuclei.

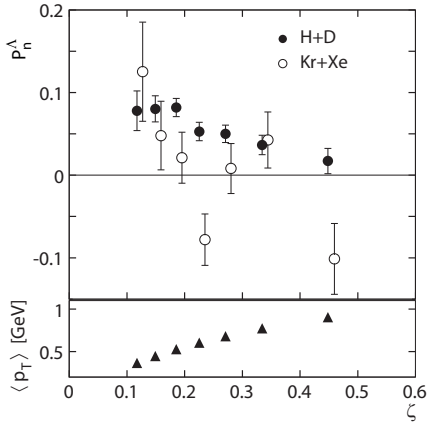

Figure 12. Dependence of the transverse polarization P_n^Λ as a function of the variable ζ.

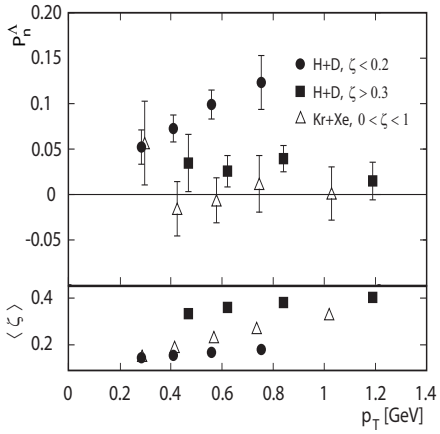

Figure 13. Dependence of the transverse polarization P_n^Λ as a function of the variable p_T.

6. New analysis for the search of pentaquark at HERMES

The earlier search at HERMES for narrow baryon states [11] excited in quasi-real photoproduction, decaying through the channel $p K_S^0 \rightarrow p \pi^+ \pi^-$, has been extended with improved decay-particle reconstruction (see figure 14), more advanced particle identification, and increased event samples [12]. The invariant mass spectra of two oppositely charged pions plotted in figure 15 show a clear K_S^0 signal peak. For comparison, the standard deviations and mean values of a single Gaussian function fit to the data together with a third-order Chebychev

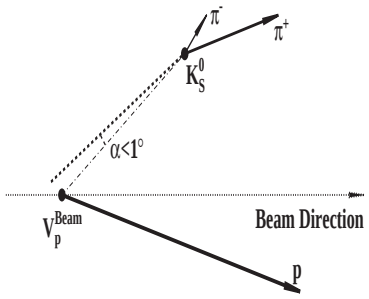

Figure 14. Diagram of the kinematic reconstruction of the decay of a Θ^+. The angle α is the difference in the direction of the K_S^0 momentum (dotted line), as given by the pion momenta, and by the vector connecting the event origin, V_p^{Beam}, with the decay of the K_S^0 (dash-dotted line).

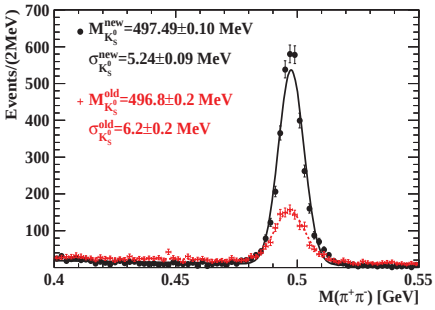

Figure 15. Invariant-mass spectra of two oppositely charged pions. The filled circles denote the analysis with data from 1998-2000 and 2006-2007, while the crosses are from the previously published analysis of the 1998-2000 data [11].

function for the background are given in this figure. As can be seen from figure 15 the new

analysis [12] has a much improved mass resolution and signal-to-noise ratio compared to that of the previous HERMES analysis [11]. The $M(pK^0_S)$ spectra for deuterium and hydrogen data taken at the HERMES experiment are shown in figure 16 and figure 17, respectively. A Voigtian (using a Gaussian with a width fixed to 6 MeV) together with two different background hypotheses was fitted to the spectrum in figure 16. The resulting curves are shown separated into signal, background contribution and also their combination. The width Γ of the Breit-Wigner function, the peak position M, and the number of signal events obtained from the fits are given in the panel. The structure observed earlier at an invariant mass of 1528 MeV shifts to 1522 MeV and the statistical significance drops to about 2σ for data taken with a deuterium target. The number of events above background is 68^{+98}_{31}(stat) $\pm$ 13(sys). Note that no such structure is observed in the hydrogen data set.

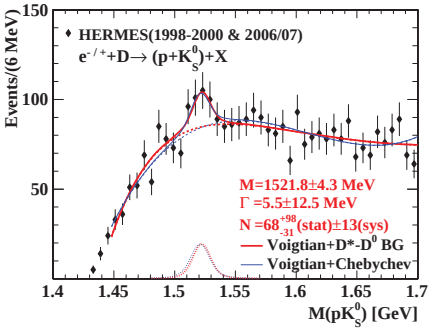

Figure 16. The $M(pK^0_S)$ spectra for deuterium data taken at the HERMES experiment.

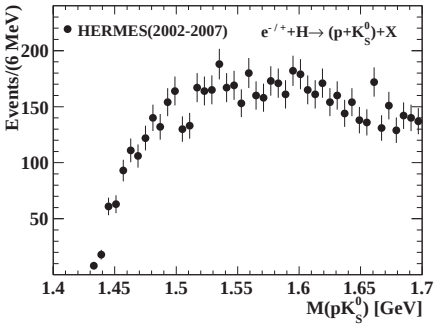

Figure 17. The $M(pK^0_S)$ spectra for hydrogen data taken at the HERMES experiment.

Acknowledgments
I would like to thank the organizers for their support and for a very interesting conference.

References

[1] Sivers D W 1990 *Phys. Rev.* D **41** 83
[2] Collins J C 1993 *Phys. Rev.* B **396** 161
[3] Airapetian A et al. 2009 *Phys. Rev. Lett.* **103** 152002
[4] Airapetian A et al. 2010 *Phys. Lett.* B **693** 11
[5] Airapetian A et al. 2007 *Phys. Lett.* B **648** 164
[6] Airapetian A et al. 2014 *Eur. Phys. J.* C **74** 3110
[7] Airapetian A et al. 2015 *submitted to Eur. Phys. J.* C, arXiv:1508.07612
[8] Goloskokov S V and Kroll P 2014 *Eur. Phys. J.* A **50** 146
[9] Airapetian A et al. 2015 *Eur. Phys. J.* C **75** 361
[10] Airapetian A et al. 2014 *Phys. Rev.* D **90** 072007
[11] Airapetian A et al. 2004 *Phys. Lett.* B **585** 213
[12] Akopov N et al. 2015 *Phys. Rev.* D **91** 057101